

Supplementary Information for

**Photo-controlled bond changes of Pt/TiO₂ for promoting overall
water splitting and restraining hydrogen-oxygen recombination**

Yajun Zhang, Hongyan Hu*, Xiaojuan Huang, Yingpu Bi*

State Key Laboratory for Oxo Synthesis & Selective Oxidation, National Engineering Research
Center for Fine Petrochemical Intermediates, Lanzhou Institute of Chemical Physics, Chinese
Academy of Sciences, Lanzhou 730000, China

E-mail: yingpubi@licp.cas.cn

Experimental section

Chemical reagents

Rutile TiO₂ nanoparticles and Chloroplatinic acid (H₂PtCl₆·6H₂O) were obtained from Sinopharm Chemical Reagent Co., Ltd, SCRC, China. All the reagents were of analytical grade and used without further purification. Deionized water (Molecular Corp., 18.25 MΩ cm) used in the synthesis was from local sources.

Preparation of Pt nanoparticles modified TiO₂.

Photocatalytic reduction method

The TiO₂ sample was immersed in 4 ml distilled water, and then 1 ml methanol and 0.26 ml H₂PtCl₆·6H₂O (19.3 mmol L⁻¹) solution were added into the solution in sequence. The mixture was irradiated by a 300 W Xe lamp (PLS-SXE300, PerfectLight Technology Co, Ltd., Beijing) with a distance of 10 cm for 5 min under ambient condition. Prior to photo-deposition, the solution was purged in advance with pure N₂ gas for 10 min to remove the dissolved oxygen. Subsequently, the preparation of sample was annealed at 450 °C for 2 h under the air condition.

Dipping method

Pt NPs was prepared via photoreduction method. And then, the Pt NPs black solution (100 μL) was loaded onto the TiO₂ surface. Finally, the preparation of sample was annealed at 450 °C for 2 h under the air condition.

Photocatalytic hydrogen evolution and hydrogen oxidation suppression test.

The photocatalytic H₂ evolution test was carried out in a glass gas-closed-circulation system (LabSolar IIIAG, PerfectLight Technology Co, Ltd. Beijing) with a top irradiation-type reaction vessel and a 300-W xenon lamp (PLS-SXE300, PerfectLight Technology Co, Ltd. Beijing). The temperature of reactant solution was maintained at 20 °C by a flow of cooling water during the test process. As-prepared Pt/TiO₂ photocatalysts were immersed into solvent were added into the reaction vessel for photocatalytic H₂ evolution test. The amounts of evolved H₂ and O₂ were monitored by an online gas chromatograph (Techcomp, 7900). No air should be present in the system after evacuation by vacuum pump.

Photoelectrochemical measurements.

Photoelectrochemical measurements was carried out in a three-electrode one-compartment photoelectrochemical cell (CHI 660d electrochemical workstation) with a quartz window to

facilitate irradiation of as-prepared photoelectrode surface. The as-prepared photoanode (actual working area of 0.1256 cm^2), a saturated calomel electrode (SCE) and a Pt wire were served as the working electrode, reference electrode and counter electrode, respectively. In addition, $0.2 \text{ mol L}^{-1} \text{ Na}_2\text{SO}_4$ (pH = 6.8) as electrolyte solution. The detail photocurrent response of as-prepared photoelectrodes materials were measured under a chopped irradiation from 300 W high-pressure short-arc xenon lamp was equipped with a cutoff filter (UVREF400) for providing ultraviolet light ($\lambda \leq 400 \text{ nm}$) as illumination source with a light intensity of 300 mW cm^{-2} , which was calibrated with a Si diode (Newport).

Characterization

The crystalline structure of the samples was identified by X-ray diffraction analysis (XRD, X'Pert PRO) using Cu $K\alpha$ radiation with the scanning rate of $0.06^\circ/\text{min}$ and 0.001° per step and the voltage as well as current of 50 kV and 50 mA. The electronic structure changes were determined by X-ray photoelectron spectroscopy (XPS, ESCALAB 250 Xi, ThermoFisher Scientific). Transmission electron microscopy (TEM) measurements were carried out by using a FEI Tecnai TF20 microscope operated at 200 kV. UV-visible diffuse reflectance spectra were performed on a UV-2550 (Shimadzu) spectrometer by using BaSO_4 as the reference.

Additional Figures and Discussions

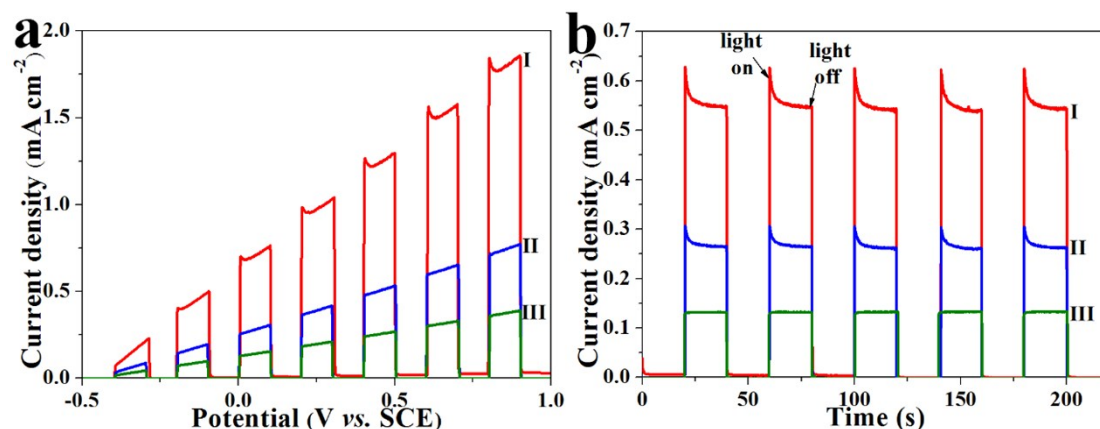


Figure S1. (a) Linear sweeping voltammograms (LSVs) in 0.2 mol L⁻¹ Na₂SO₄ electrolyte at the scan rate of 10 mV s⁻¹ at a potential range of -0.5 V to 1.0 V (vs. SCE); (b) Chronoamperometric i-t curves in 0.2 mol L⁻¹ Na₂SO₄ electrolyte at the potential of 0 V (SCE) under chopped light irradiation with 20 s on or off cycles. (I: P-Pt/TiO₂; II D-Pt/TiO₂ and III: Pure TiO₂)

Additional discussion:

To illustrate the distinction of as-prepared photocatalysts, the photoelectrochemical performance was investigated in 0.2 mol L⁻¹ Na₂SO₄ electrolyte. Figure S1a compares the linear sweeping voltammograms (LSVs) of as-prepared photoelectrodes at the scan rate of 10 mV s⁻¹. As shown in Figure S1a, the dark scans collected in the potential range reveal that the photocurrent densities of as-prepared samples are almost negligible, with small background current density of ~10⁻¹⁰ A cm⁻². Under the light irradiation, all of samples exhibit significantly enhancement of photocurrent response density, due to efficient photocharge separation and migration. More particularly, the P-Pt/TiO₂ exhibits much higher photocurrent response than that of pure TiO₂ and D-Pt/TiO₂ samples. For detailed comparison, the steady-state Chronoamperometric i-t curves were measured and recorded under the chopped light illumination at a constant potential of 0 V (vs. SCE) (Figure S1b). Compared to the photoresponse activity of pure TiO₂ (0.13 mA cm⁻²), the maximum photocurrent density of P-Pt/TiO₂ reaches as high as ~0.55 mA cm⁻² at a bias potential of 0 V (vs. SCE) and is very stable even after 5 periodic cycles, which is consistent with values obtained from LSV curves of P-Pt/TiO₂.

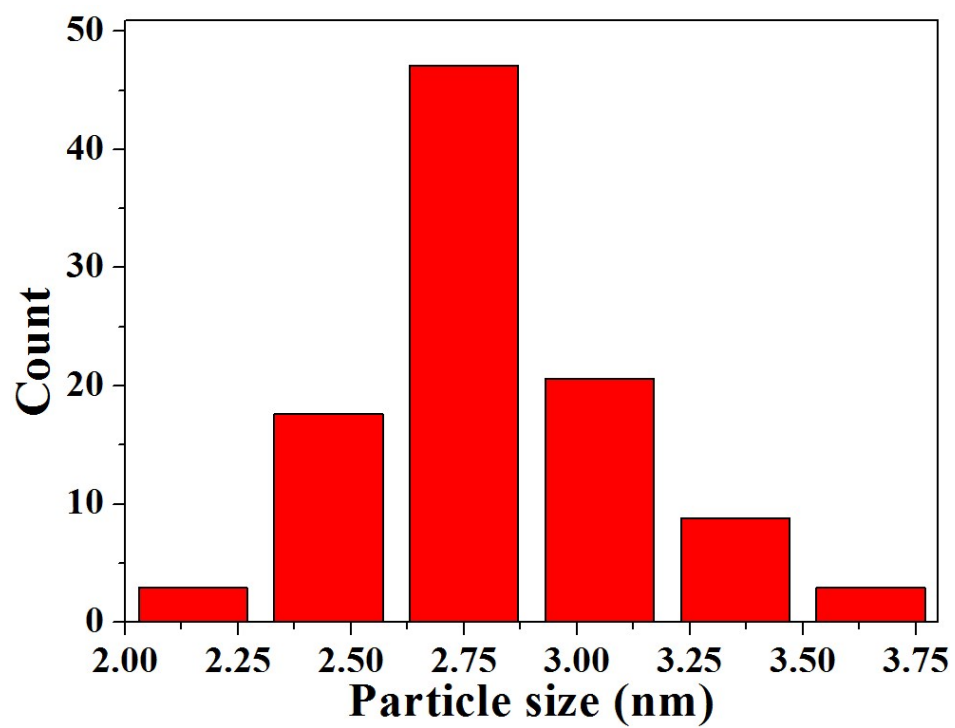


Figure S2. Pt particles size distribution

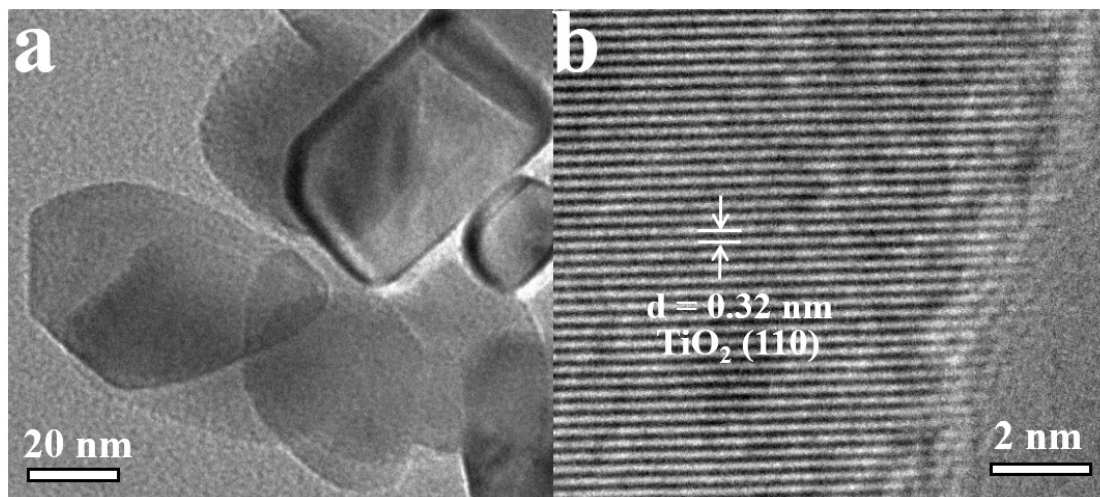


Figure S3. TEM and HRTEM images of pristine TiO₂

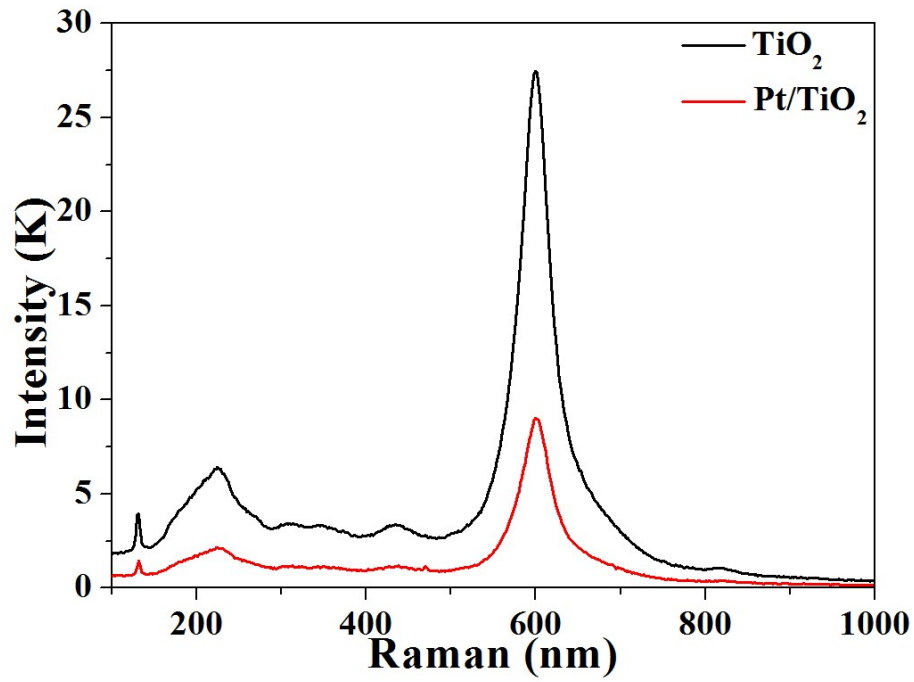


Figure S4. Raman spectra of pure TiO_2 and P-Pt/ TiO_2

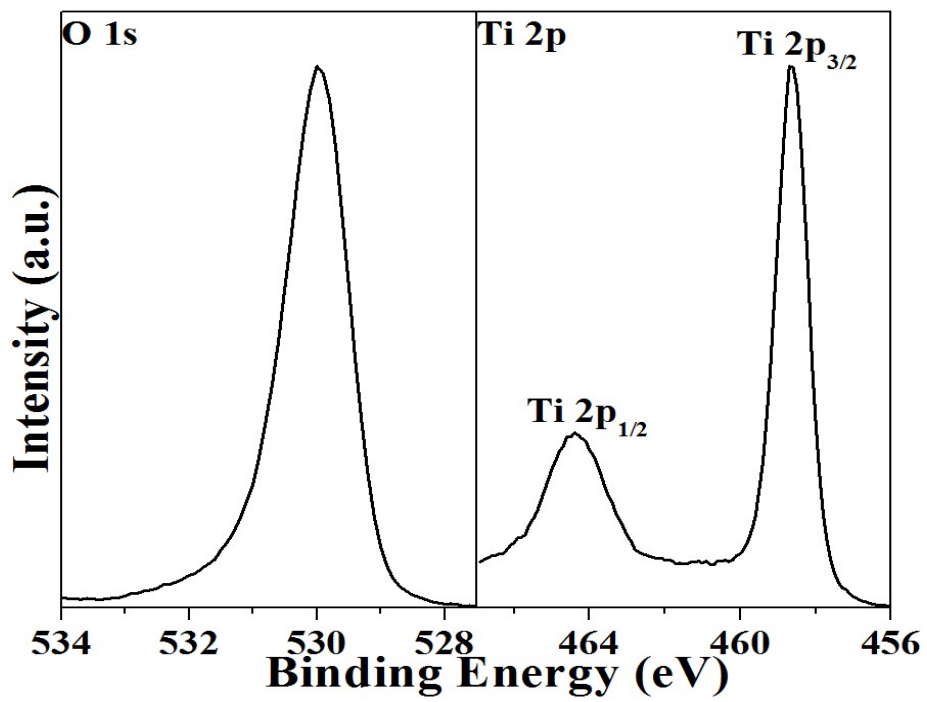


Figure S5. XPS spectra of pure TiO_2

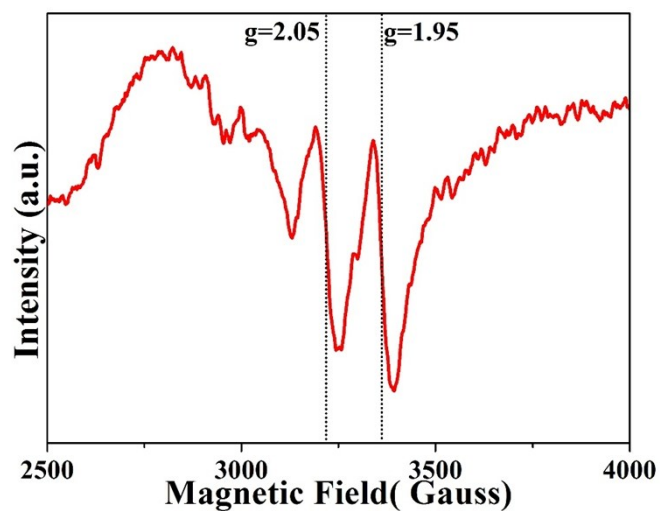


Figure S6. EPR spectra of TiO₂

Additional discussion:

The oxygen vacancies were confirmed in pure TiO₂ by low-temperature electron paramagnetic resonance (EPR). As shown in Figure S6, the characteristic signals at $g = 1.95$ and $g = 2.05$ were detected. According to the literatures¹⁻³, the paramagnetic Ti³⁺ has a g -value of 1.94-1.99 and oxygen vacancies at $g = 2.05$. Based on the above result, we can confirm that the enriched “free electrons” may transfer from O vacancies to Ti atom in pure TiO₂ under the ground state.

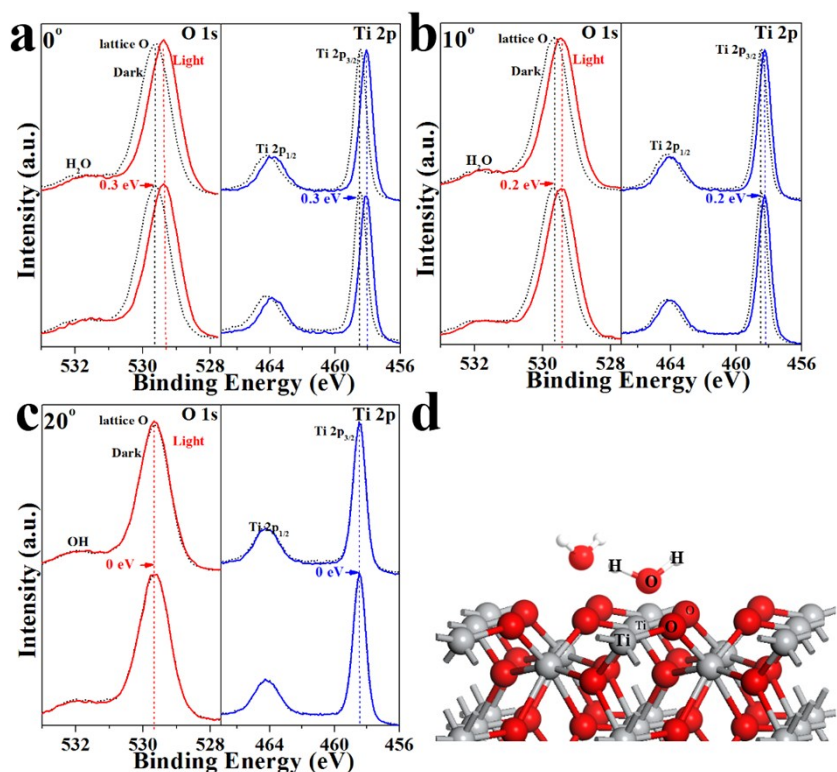


Figure S7. The SI-XPS spectra of H₂O/TiO₂ with different angles (a-c), and schematic ball model of TiO₂ surface with H₂O absorption.

Additional discussion:

As shown in Figure S7, in the case of pristine TiO₂, no evident bond changes of Ti 2p and O 1s peak have been detected with different angles, and the BE offsets in Ti and O atoms have been gradually reduced and finally disappeared, which should be suffered from the formation of OH group with strong electron-attracting ability on surface Ti atoms. This result may give the reasonable explanations for the inactivity of TiO₂ alone for overall water splitting.

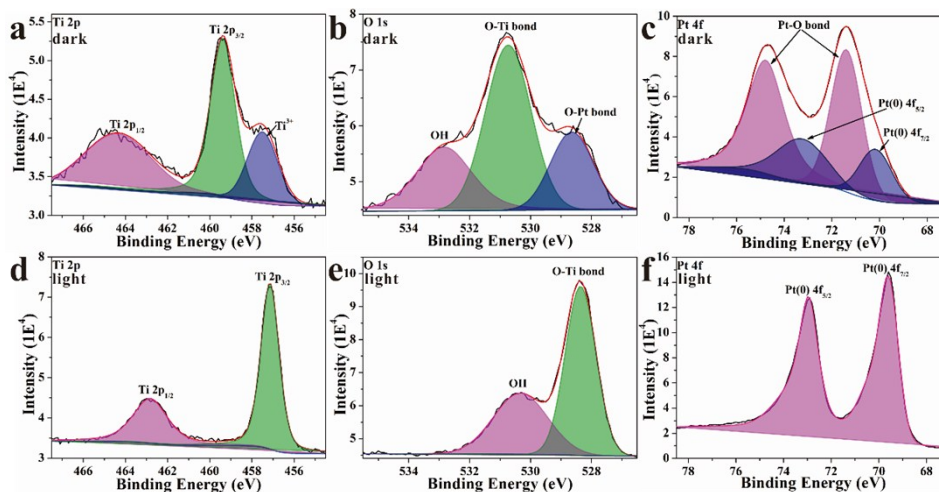


Figure S8. The XPS-peak-differentiation-imitating analysis spectra of P-Pt/TiO₂ at the angle of 20° under the dark condition (a-c) and light condition (d-f), respectively.

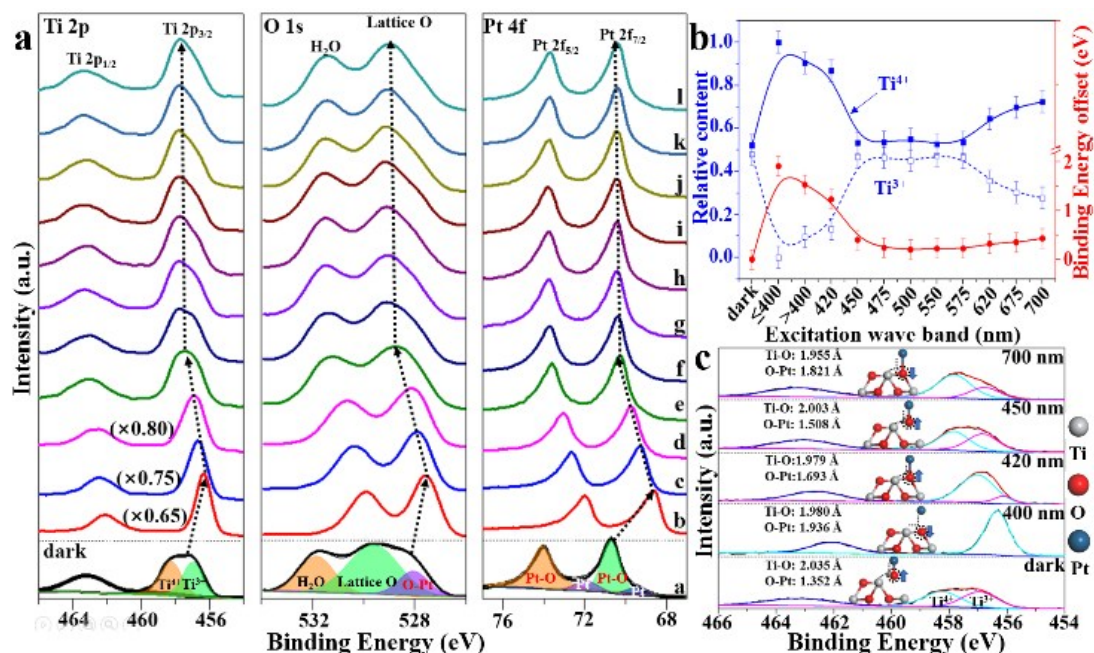


Figure S9. Wavelength-dependent electronic structure and atomic bond changes of P-Pt/TiO₂. a: AR-SI-XPS spectra of P-Pt/TiO₂ at 30° with different wavelength ranges (a: dark; b: ≤400 nm; c: >400 nm; d: 420±15 nm; e: 450±15 nm; f: 475±15 nm; g: 500±15 nm; h: 550±15 nm; i: 575±15 nm; j: 620±15 nm; k: 675±15 nm; l: 700±15 nm); b: blue curve: Wavelength ranges-dependent relative content of Ti⁴⁺ and Ti³⁺, respectively. The data points derived from the rationally fitting of SI-XPS spectra of Ti 2p_{3/2} peaks from UV to infrared light; red curve: excitation wave band-dependent BE offset of Ti 2p; c: the XPS-peak-differentiation-imitation spectra of Ti⁴⁺ and Ti³⁺, respectively, and their possible model structure and bond length.

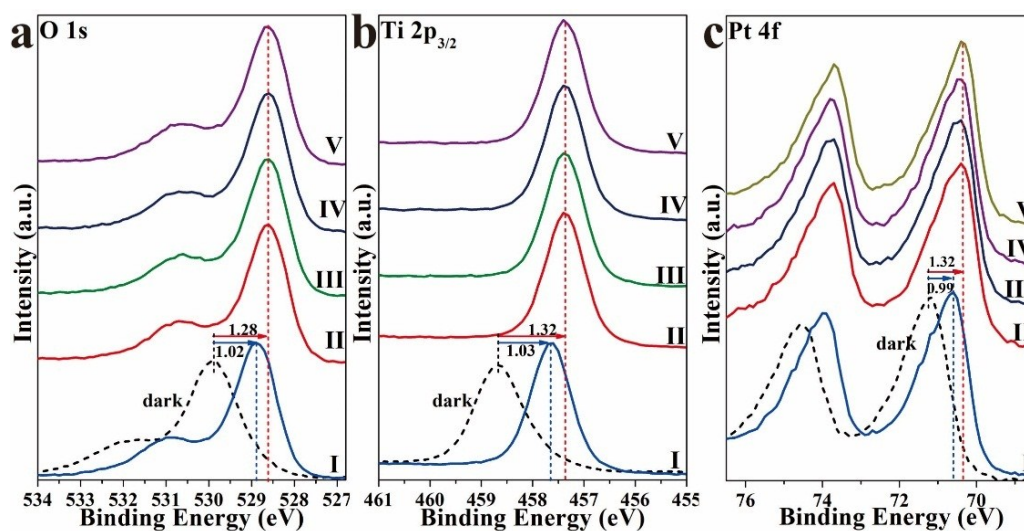


Figure S10. The SI-XPS spectra of P-Pt/TiO₂ with different light condition. (I: visible light; all wavelength; II: 42.8 mW cm⁻²; III: 34.2 mW cm⁻²; IV: 28.2 mW cm⁻²; V: 21.4 mW cm⁻²)

Additional discussion:

Up to now, Pt/TiO₂ is known to be only ultraviolet (UV)-light responsive owing to the large bandgap structure (rutile TiO₂: 3.0 eV)³. However, the effect of photon energy below this bandgap

on the electronic structure and atomic bond is still unclear. To break through this limitation, the electron transfer and bond changes under the light irradiation with different wavelengths have been further studied under the angle of 30° for further increasing the surface sensitivity. As shown in Figure S9a, under the ground states, more evident peaks of Ti³⁺ and Pt-O bond in the SI-XPS spectra have been observed, owing to the main contribution of surface atoms. However, when incident light with different wavelengths was employed, distinct BE offsets and bond change features have been achieved. To further show the BE offsets as well as bond changes, the SI-XPS spectra of Ti 2p peaks from UV to infrared light have been rationally fitted and summarized in Figure S9b and S9c. More specifically, in the case of UV-light (400nm), the typical peaks of Ti³⁺ and O-Pt bond completely disappeared in the SI-XPS spectra, and significant BE offsets for O 1s, Ti 2p and Pt 4f peaks have also been observed. For visible light from 400 to 450 nm, the peaks of Ti³⁺ and O-Pt bond in the SI-XPS spectra have been significantly increased, and BE offsets has been evidently decreased. Interestingly, in the case of 450-575 nm, no evident change for both BE offsets and bond could not be detected, indicating that the P-Pt/TiO₂ photocatalyst could not excited by the photon energies from 2.1 to 2.7 eV. However, further increasing the wavelength ranges from 620 to 700 nm, the evident bond changes have been detected again, which should be attributed to oscillatory features of Ti-O and Pt-O bond resulted from the infrared thermal-effects. This phenomenon clearly reveals that the photon energy is not exclusive for determining the bond changes. Moreover, the light intensity has been rationally adjusted while kept the wavelength ranges, and no any change of BE offsets and bond have been observed in the SI-XPS spectra (Figure S10). Accordingly, these reversible bond-change features under the ground state and excitation state are the intrinsic nature of Pt/TiO₂, which is independent of incident light intensity and only depended on excitation-wavelengths.

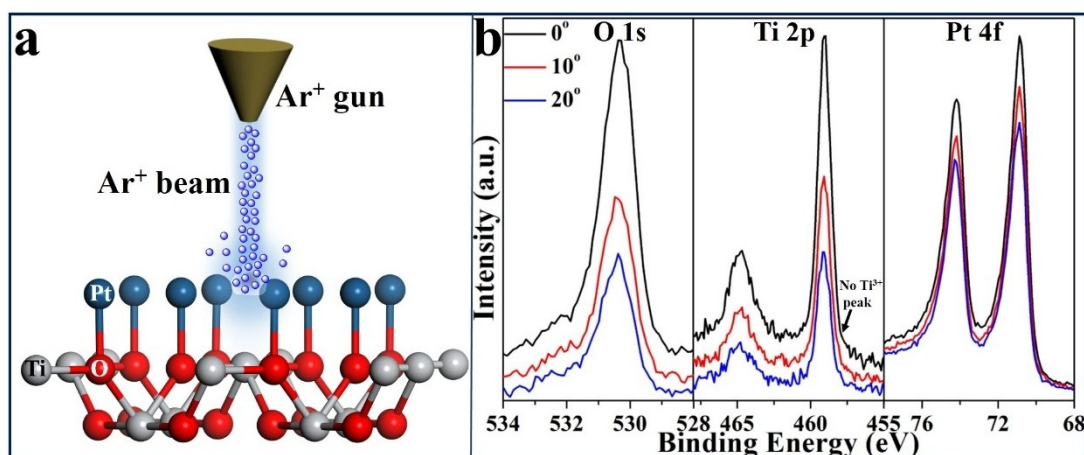


Figure S11. The evidence of Pt atom occupies on lattice O atom site of P-Pt/TiO₂. The ball-stick model (a) and XPS spectra for Ar⁺ sputtered P-Pt/TiO₂ surface under the change angle condition (b). Acceleration voltage of Ar ion is 2000 eV.

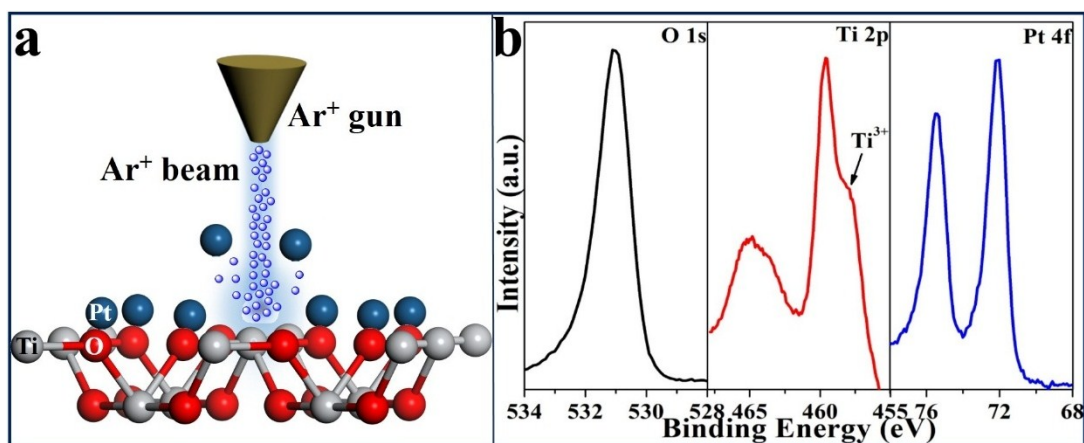


Figure S12. The evidence of Pt atom occupies on lattice O atom site of D-Pt/TiO₂. The ball-stick model (a) and XPS spectra for Ar⁺ sputtered D-Pt/TiO₂ surface (b). Acceleration voltage of Ar ion is 2000 eV.

Additional discussion:

To prove the Pt atom occupies activity site, the experiment for Ar⁺ sputtered as-prepared samples surface was carried out (Figure S11 and S12). After Ar⁺ sputtered P-Pt/TiO₂ surface (Figure S11a), the Ti³⁺ peak and other variations peak have not appeared in the multiangle spectrum (Figure S11b), indicating that Pt atoms have been bound with surface O atom of TiO₂ to form Pt-O bond, which can efficiently protect internal lattice O atom. This result can further confirm that SI-XPS results of P-Pt/TiO₂ (Figure 4). However, when Ar⁺ sputtered surface of D-Pt/TiO₂ (Figure S12a), the Ti³⁺ peak appear in the Ti 2p region at low binding energy (Figure S12b). This result can further explain that the simple physical contact cannot form efficient chemical bond changes and increase transfer ability of photocharge over photocatalyst surface.

Additional Formula and calculative process

According to the Doniach-Sunjić profile⁴ (eq.1), Pt 4f_{7/2} peak can be fitted in Table S1:

$$Y(E) = \frac{\Gamma(1 - \alpha)}{((E - E_0)^2 + \gamma^2)^{(1-\alpha)/2}} \cos\left\{\frac{\pi\alpha}{2} + (1 - \alpha) \tan^{-1}\left(\frac{E - E_0}{\gamma}\right)\right\} \quad (1)$$

Where $Y(E)$ is the registered intensity of XPS peak, E_0 is binding energy, Γ is the gamma function, γ is the lifetime broadening, and α is the asymmetry parameter.

Furthermore, experiment asymmetry index (A) can also be calculated using the following equation⁵:

$$A = 1 - \frac{fwhm_L}{fwhm_R} \quad (2)$$

Where $fwhm_L$ is the peak width at the half-maximum, measured only for higher BE side of the peak only, and $fwhm_R$ is the peak width at the half-maximum, measured only for lower BE side of the peak. It measures the peak departure from the symmetric form and is completely independent of the line shape used for deconvolution. Thus, the peak with an ideal symmetry would have $A=0$, and the more asymmetric peak, the higher A, similar as α , but independent of the assumed line shape.

Additional Table and discussion

Table S1. Details of Pt 4f peak deconvolution and asymmetry analysis.

| Sample name | Pt 4f _{7/2} BE | α (eq.1) | A(eq.2) | Pt 4f _{7/2} BE | α (eq.1) | A(eq.2) |
|-----------------------|-------------------------|-----------------|---------|-------------------------|-----------------|---------|
| | dark | | | Light | | |
| P-Pt/TiO ₂ | 71.38 | 0.50 | 0 | 69.51 | 0.25 | 0.21 |
| D-Pt/TiO ₂ | 70.85 | 0.30 | 0.29 | 70.85 | 0.30 | 0.29 |

To explore the electronic structure changes of as-prepared Pt/TiO₂ samples, the asymmetry analysis of Pt 4f peak have been performed (detail calculative process and formula are described as above). As shown in Table S1, under the dark condition, α parameter from eq 1 is close to 0.28, whereas the result for P-Pt/TiO₂ under the ground state shows higher asymmetry (0.5) than that of other Pt/TiO₂. Herein, A and α have been determined with a precision of ± 0.01 , which confirm that there is a small change in the asymmetry of Pt/TiO₂, and no significant change in case of D-Pt/TiO₂. However, the significant asymmetry changes of Pt 4f in P-Pt/TiO₂ have occurred under the light irradiation, indicating that the light-induced electron density states change on photocatalyst surface, which highly consistent with the result of SI-XPS for P-Pt/TiO₂.

Reference

- 1 M. Wajid Shah, Y. Zhu, X. Fan, J. Zhao, Y. Li, S. Asim, C. Wang, *Sci. Rep.*, 2015, **5**, 15804.
- 2 H. J. Zhai, L. S. Wang, *J. Am. Chem. Soc.*, 2007, **129**, 3022.
- 3 S. Wendt, P. T. Sprunger, E. Lira, G. K. Madsen, Z. Li, J. O. Hansen, J. Matthiesen, A. Blekinge-Rasmussen, E. Laegsgaard, B. Hammer, F. Besenbacher, *Science*, 2008, **320**, 1755.
- 4 S. Doniach, M. Sunjic, *J. Phys. C*, 1970, **3**, 285.
- 5 A. Lewera, L. Timperman, A. Roguska, N. Alonso-Vante, *J. Phys. Chem. C*, 2011, **115**, 20153.